

In Situ Spectroelectrochemical and Rotating Ring–Disk Electrode Studies on the Initial States in the Reductive Electropolymerization of Poly(*p*-phenylene vinylene)

P. Damlin,^{†,§} C. Kvarnström,^{*,†} A. Petr,[‡] A. Neudeck,[‡] L. Dunsch,[‡] and A. Ivaska[†]

Process Chemistry Group, c/o Laboratory of Analytical Chemistry, Åbo Akademi University, FIN-20500, Turku-Åbo, Finland; Group of Electrochemistry and Conducting polymers, Institute of Solid State and Materials Research Dresden, D-01107 Dresden, Germany; and Graduate School of Materials Research, Åbo Akademi University, FIN-20500, Turku-Åbo, Finland

Received October 18, 2001; Revised Manuscript Received April 8, 2002

ABSTRACT: The reductive coupling reactions in electrochemical polymerization of poly(*p*-phenylene vinylene) (PPV) have been studied by in situ UV–vis spectroscopy using lithographic galvanic microstructured metal foils (LIGA structure) as the working electrode, in situ UV–vis–ESR spectroscopy, and by the rotating ring–disk electrode (RRDE) technique. The polymer film was synthesized by electrochemical reduction of the monomer $\alpha,\alpha,\alpha',\alpha'$ -tetrabromo-*p*-xylene (**1**) in dimethylformamide using tetraethylammonium tetrafluoroborate as the supporting electrolyte. The results show that the reduction of monomer **1** takes place in two steps. The first step is a two-electron reduction process leading to formation of intermediates that stay in solution without precipitation onto the electrode surface. The second two-electron reaction of these intermediates produce oligomers which precipitate onto the surface of the electrode. It was observed that the electrode material, cell design, and temperature have a marked influence on the value of the peak potential of the second reduction reaction.

1. Introduction

Conjugated polymers are characterized by a highly delocalized π -electron structure lying along the polymer backbone. When doped, these materials can display even metallic conductivities for to which they have attracted much interest. Poly(*p*-phenylene vinylene) (PPV) is an example of these semiconducting polymers. It was with PPV that polymer electroluminescence was first demonstrated in 1990.¹ A common way to obtain insoluble PPV layers is the sulfonium precursor route in which conversion of the precursor into PPV is accomplished by thermal elimination of the sulfonium groups.^{2,3} This elimination reaction is a crucial step in the synthesis because traces of unconverted material can cause defects in the polymer which significantly effect the performance of the final material.

The electrochemical synthesis route offers direct and easy material formation without need of the heat treatment step used in chemical synthesis of PPV. By tuning the electrochemical parameters, used for film formation, one may also control film growth to a much greater degree. Electrochemical polymerization of conducting polymers is usually done by anodic oxidation of the monomer material. Such processes have been extensively studied and a generally accepted mechanism of electropolymerization of polyheterocycles is radical–radical coupling followed by chain propagation.⁴ Results reported on conducting polymers obtained by in situ differential ellipsometry,⁵ rotating ring–disk electrode,⁶ and microelectrodes⁷ have shown that oxidative electropolymerization starts with the formation of oligomers in solution. Presence of soluble intermediates prior to

the polymer formation was confirmed in all these studies. In the case of reductive electropolymerization only a few reports exists, mostly involving the electroreduction of 1,4-dibromobenzene nickel complexes for preparing poly(*p*-phenylene) (PPP).⁸

In this work we will focus on obtaining PPV films produced by electrochemical reduction of $\alpha,\alpha,\alpha',\alpha'$ -tetrabromo-*p*-xylene in dimethylformamide (DMF) using potential cycling.⁹ In previous work our group has studied how different parameters such as polymerization potential, type of solvent, and electrolyte salt and water content in the solvent affect both the growth of PPV in the polymerization reaction and the properties of the final polymer.^{9,10} Very few results describing electrochemical reduction of organic aliphatic halides have been reported in the literature. Covitz¹¹ and Gilch¹² were the first to study the electrochemical reduction of α,α' -dihalo-*p*-xylenes. In ref 13, the catalytic reduction of vicinal dihalides have been studied. Utley et al. synthesized poly-*p*-xylene polymers by electrochemical reduction from 1,4-bis(bromomethyl)arenes on mercury electrode.¹⁴ The same group also used the same method for the synthesis of PPVs from 1,4-bis(dihalomethyl)arenes. In refs 11, 12, and 14, the reduction reaction was suggested to proceed via quinodimethane intermediates according to reaction Scheme 1. However, no thorough study of the different steps given in Scheme 1 has to our knowledge been reported. Knowing the chemical characteristics of the intermediates is crucial for understanding the mechanism of the complex electropolymerization process.

The aim of the present work is to study and identify the intermediates formed during electrochemical reduction of $\alpha,\alpha,\alpha',\alpha'$ -tetrabromo-*p*-xylene by the rotating ring–disk electrode (RRDE) and in situ spectroelectrochemical (UV–vis and/or ESR) methods. By using the combined spectroelectrochemical UV–vis–ESR technique, one gains the possibility of obtaining structural

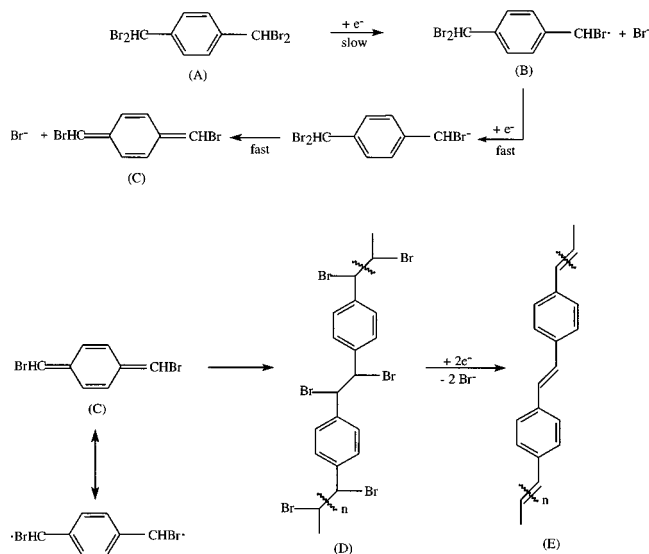
* Corresponding author. E-mail: ckvarnst@abo.fi.

[†] Process Chemistry Group, Åbo Akademi University.

[‡] Institute of Solid State and Materials Research Dresden

[§] Åbo Akademi University, Graduate School of Materials Research.

Scheme 1. Reaction Mechanism for the Monomer $\alpha,\alpha,\alpha',\alpha'$ -Tetrabromo-*p*-xylene (A) upon Electroreduction



information about both the paramagnetic and diamagnetic species in an electrochemical reaction.¹⁵

2. Experimental Section

2.1. Chemicals. Electrochemical polymerization of PPV was performed in dimethylformamide (DMF, Lab-Scan) solutions containing 0.1 M tetraethylammonium tetrafluoroborate ((TEA)-BF₄, Aldrich) as the supporting electrolyte and various concentrations of the monomer material $\alpha,\alpha,\alpha',\alpha'$ -tetrabromo-*p*-xylene (**1**, Tokyo Kasei). The monomer material, **1**, was used as received. The supporting electrolyte, (TEA)BF₄, was dried at 80 °C for 1 h under vacuum conditions before use. Before use, DMF was purified by drying over activated aluminum oxide (Al₂O₃, Aldrich).

2.2. Apparatus. A rotating ring-disk (Pt-Pt) electrode (RRDE) system (model 636) combined with a Bi-potentiostat (model 366A) and a X-Y recorder (model RE01151, all from EG&G PAR) were used in the RRDE experiments. The dimensions for the RRDE were $r_1 = 0.2285$ cm, $r_2 = 0.2465$ cm and $r_3 = 0.269$ cm where r_1 is the platinum disk radius and r_2 and r_3 are the inner and outer platinum ring radii, respectively. In the RRDE experiments, a glassy carbon (GC) rod served as the auxiliary electrode and a silver wire coated with silver bromide was used as a pseudo-reference electrode (+0.38 V vs SCE vs ferrocene in 0.1 M (TEA)BF₄-DMF). All potentials are referred to this reference electrode otherwise differently stated. A one-compartment three-electrode glass cell was used in the electrochemical RRDE experiments.

The in situ UV-vis experiments were performed in a spectroelectrochemical three-electrode flow cell based on a screw joint of two Teflon parts to hold the LIGA electrode structure.¹⁶ Quartz rods in the bore of the center of the Teflon parts conduct the light beam through the cell. The Au LIGA structure was used as the working electrode. Inside the electrolyte inlet of the cell, a silver wire coated with silver bromide was used as pseudo-reference electrode and a platinum wire in the electrolyte outlet was used as the counter electrode. The optical absorption spectra were recorded in the wavelength range from 200 to 1100 nm with an UV-vis diode array Instaspec II spectrometer (LOT Oriel, Darmstadt, Germany) running in the kinetic mode with external triggers. The 75 W Xe lamp and the spectrometer were connected by light fibers to the LIGA cell.

In the UV-vis-ESR measurements an ESR 300 E X-band (Bruker) spectrometer and the UV-vis instrument described above were used in a combined manner. The electrochemical flat cell used in the electrochemical ESR investigations has been described earlier.¹⁵ A Pt mesh of dimension 5 mm × 4

mm was used as the working electrode. The Pt mesh was made from a wire of 0.06 mm diameter with 1024 meshes per cm². A AgCl-coated wire within a capillary was used as the reference electrode. A Pd-sheet counter electrode was placed below and a Pt-wire counter electrode was situated above the flat part of the ESR cell. This construction with two counter electrodes was used in order to avoid distortion of the current-voltage curves (ohmic drop). In the electrochemical measurements a PC controlled potentiostat PG 285 (HEKA Lambrecht, Germany) was used. The in situ UV-vis-ESR spectroelectrochemical measurements were controlled by a homemade program driving the potentiostat by AD-DA plug-in boards and triggering the ESR and UV-vis spectrometers.

2.3. Procedure. In the RRDE experiments the potential of the disk (E_D) was maintained at stepwise increasing constant potentials between 0 and -2.3 V. Simultaneously a current-potential curve was recorded at the ring by cycling the potential between -0.7 and +1.4 V. A scan rate of 50 mV/s and a rotation rate of 600 rpm were used. Furthermore, the changes in the disk (i_D) and ring currents (i_R) during a potential scan of the disk between 0 and -2.3 V using 50 mV/s as scan rate were recorded. In these experiments the ring potential (E_R) was maintained at +1.0 or +1.3 V and the rotation rate was altered between 300 and 2000 rpm. In the RRDE experiments, the concentration of the monomer material **1** was 0.05 M in 0.1 M (TEA)BF₄-DMF solution. The RRDE was polished mechanically with Al₂O₃ powder (grain size 0.3 and 0.05 μ m) before each experiment. Oxygen was removed from the solutions by purging with dry nitrogen for several minutes before the measurements. During the measurements the solutions were blanketed with a stream of nitrogen.

The collection efficiency, N , of the RRDE system was determined using an aqueous solution with 1 mM K₄Fe(CN)₆ in 0.1 M KCl. The E_D was cycled between -0.1 and +0.6 V using 50 mV/s as the scan rate and a rotation rate of 600 rpm. Both the i_D and i_R were recorded as functions of E_D . The E_R was held at a constant potential value of -300 mV, enough to reduce the ferricyanide formed at the disk. N could then be obtained from the ratio i_R/i_D . The experimentally obtained RRDE collection efficiency of our system was found to be 0.2; i.e., 20% of the product generated at the disk is collected at the ring. This value is in good agreement with the theoretical collection efficiency of 0.216 calculated by using the electrode dimensions.¹⁷

In the UV-vis experiments using the LIGA cell, the intermediates formed during electrochemical polymerization of PPV were studied by applying a constant potential of -1.0 V for 2 s to the cell and then recording the changes in absorbance vs time. Solutions containing 0, 2, 4, or 6 mM of monomer **1** with 0.1 M (TEA)BF₄ in DMF were used in the experiments.

The effect of temperature on the absorbance response of the intermediate products was studied by performing experiments both at room temperature, ca. 23 °C, and at -10 °C. At the same time the change in the intensity of the ESR signal was measured. In these UV-vis-ESR experiments a thin layer spectroelectrochemical cell with a Pt mesh as working electrode was used. The potential was cycled between 0 and -2.3 V in a 0.05 M solution of monomer **1** with 0.1 M (TEA)BF₄ in DMF. In the experiments performed at a temperature of -10 °C the potential was cycled between 0 and -1.3 V.

3. Results and Discussion

3.1. Mechanism of PPV Formation. 3.1.1. RRDE Measurements. Figure 1 shows the current response during electropolymerization of monomer **1** on a Pt disk electrode (0.07 cm²) by potential cycling between 0 and -2.3 V using 50 mV/s as the scan rate (first cycle). Two reduction processes can be observed at around -1.4 and -1.9 V. From earlier studies using EQCM, FTIR, and Raman spectroscopy techniques, it was found that precipitation of the PPV film onto the working electrode

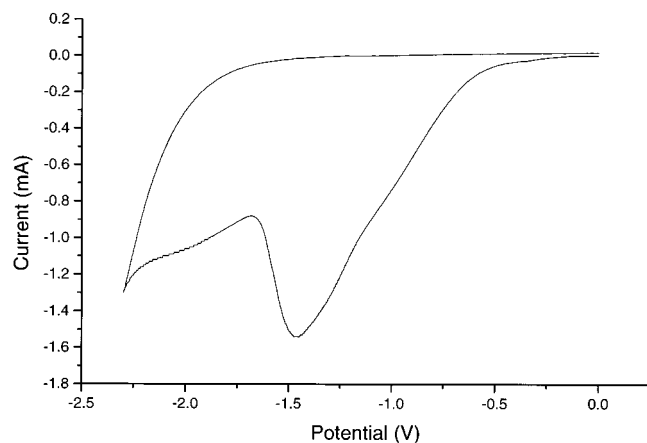


Figure 1. Electrochemical reductive polymerization of PPV by potential cycling between 0 and -2.3 V on a Pt-disk electrode in a 0.1 M (TEA)BF₄-DMF solution containing 0.05 M monomer **1** using a 50 mV/s scan rate.

takes place only after reaching -1.6 V.^{10,18–19} The current response observed in Figure 1 before reaching this potential value is therefore due to formation of intermediate species involved in electropolymerization of PPV. Furthermore, no current peak is seen for the reverse process, also indicating that the products formed in the potential range -0.5 to -1.6 V undergo a rapid follow-up reaction. The intermediate products giving rise to the current response before reaching the potential of -1.6 V will be further studied by the RRDE technique.

In the RRDE study, the disk electrode was kept at different constant potentials between 0 and -2.3 V and current–voltage curves were recorded at the ring electrode. This allows identification of free intermediates in solution formed at the disk. Because of the electrode rotation the intermediates formed at the disk are hydrodynamically transported across the insulating gap toward the ring where they can be oxidized. Such i_R vs E_R curves obtained during polymerization of monomer **1** by applying constant potentials between 0 to -0.9 V and -1.0 to -2.3 V onto the disk can be seen in Figure 2, parts a and b, respectively. Observe the different current scales used in Figure 2, parts a and b (0.01 and 0.02 mA/cm). The E_R was scanned between -0.7 and $+1.4$ V.

No significant current is observed at the ring until the disk reaches a potential of about -0.6 V, a potential at which an increase in current was also obtained in Figure 1. At E_D lower than -0.6 V the current response from the ring consists of two well-defined waves with $E_{R,1/2}$ at $+0.78$ and $+1.2$ V. The $E_{R,1/2}$ of the first oxidation process shifts to less positive potentials ($+0.9$ to $+0.78$ V) with increasing negative potential applied to the disk. The $E_{R,1/2}$ for the second oxidation process at $+1.2$ V remains constant although the E_D is changed. The current of the two oxidation processes also depends on the potential applied onto the disk electrode as can be seen from Figure 2, parts a and b. The ring current for the two oxidation waves increases when potentials in the ranges -0.6 to -1.0 V and -1.7 to -2.3 V are applied to the disk. In Figure 1, an increase in the current response could also be observed in these potential ranges. A current decrease can, however, be observed on the ring when potentials between -1.2 and -1.6 V are applied on the disk.

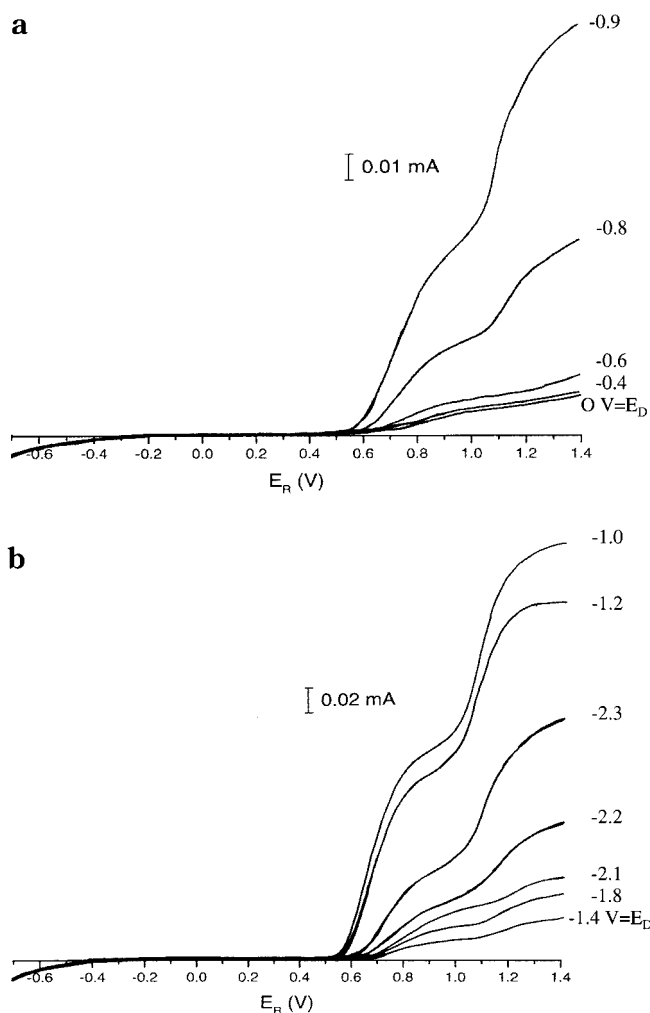


Figure 2. Ring current vs ring potential curves obtained at different constant negative disk potential values (E_D). The E_D was held at constant potentials between (a) 0 to -0.9 V and (b) -1.0 to -2.3 V. The E_R was cycled between -0.7 and $+1.4$ V in a 0.1 M (TEA)BF₄-DMF solution containing 0.05 M monomer **1**. The scan rate was 50 mV/s, and a rotation rate of 600 rpm was used.

From the structure of monomer **1** (A) shown in Scheme 1, it can be seen that there are four bromine atoms, two of each at the attached carbon atoms. These bromine atoms have to be removed during the reductive potential cycle in order to get PPV as the final material. By energy-dispersive X-ray analysis (EDXA) of PPV, it was shown that no bromine is present in the electrochemically polymerized film.⁹ In the RRDE experiments we would then expect to see oxidation at the ring from the expelled Br[−] ions. This oxidation can be observed in two steps in Figure 2 at $+0.78$ and at $+1.2$ V which is in accordance with the values reported in reference.²⁰ The dependence of the i_R on the E_D indicates that cleavage of the carbon–bromine band takes place in two steps. The first cleavage of bromine during the reduction of monomer **1** can be observed when applying potentials between -0.6 and -1.0 V to the disk. The intermediate product formed in this process is oxidized at $+0.78$ V at the ring. When potentials higher than -1.7 V are applied to the disk the intermediate product is further reduced, leading to splitting of the remaining bromine atoms indicated by the increase in i_R observed again at $+1.2$ and $+0.85$ V. From these experiments, it can then be concluded that four electrons in all must be consumed when reducing monomer **1** (A). In the first reduction

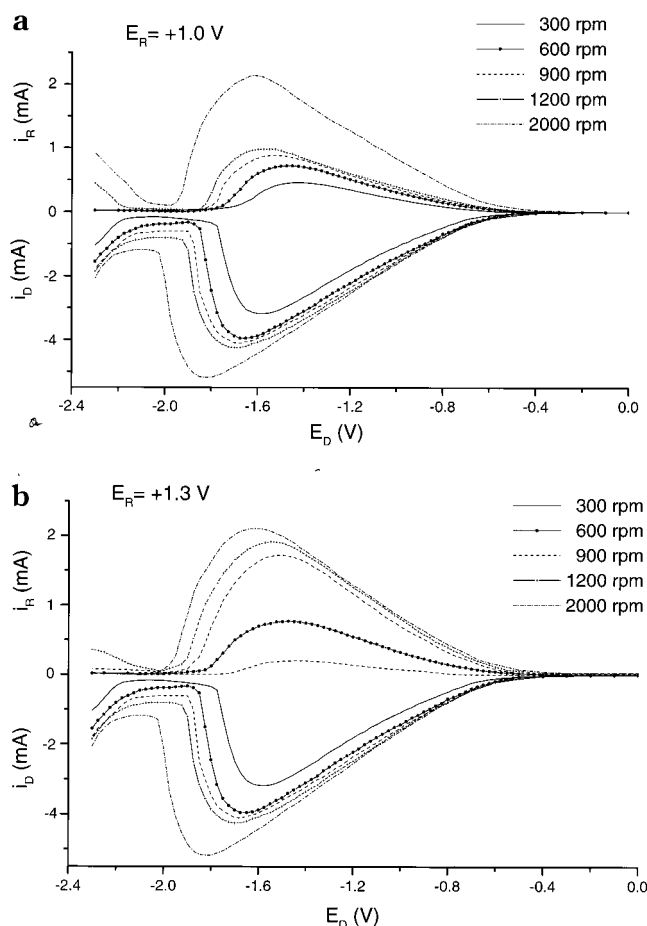


Figure 3. Disk (i_D) and ring (i_R) currents obtained during reduction of monomer **1** (0.05 M) in 0.1 M (TEA)BF₄-DMF by potential scanning between 0 and -2.3 V. The rotation rate was varied between 300 and 2000 rpm; the scan rate was 50 mV/s. E_R was set at (a) $+1.0$ and (b) $+1.3$ V.

wave two electrons are used, leading to the intermediate brominated quinodimethane (C) in accordance with Scheme 1. In the following experiments the bromine elimination will be further studied in order to find the reduction mechanism behind the current waves observed in Figure 1.

Parts a and b of Figure 3 show the variation of the i_D and the i_R recorded during the negative sweep between 0 and -2.3 V of the disk as a function of rotation rates. The E_R was set at $+1.0$ (a) or $+1.3$ V (b), the potentials at which the two oxidation waves could be observed in Figure 2. From Figure 3, parts a and b, it can be seen that both i_D and i_R increase with increasing rotation rate. The peak potential is also dependent on the rotation rate showing a negative shift with increasing rotation rates. Because of this potential shift the scan is reversed close to the second peak potential (compare with Figure 1). A nucleation loop is therefore observed on the reverse sweep of the first cycle (reverse scan not shown in Figure 3) which has been interpreted as the start of the nucleation process of the corresponding polymer.^{21,22}

When visually inspecting the PPV film formed on the disk electrode it was observed that the growth of the film was not uniform. The center of the electrode, i.e., the less perturbed zone was covered with a thicker layer of polymer. The enhanced transport of intermediates away from the electrode surface upon rotation of the electrode will greatly inhibit even deposition of

polymer on the disk. These findings give further evidence for the existence of intermediate species in the polymerization reaction.^{6,23}

To obtain the collection efficiency, N , for the products oxidized at the ring at $+1.0$ and $+1.3$ V, values for i_R and i_D from Figure 3 in the potential range -0.47 to -1.1 V at a rotation rate of 600 rpm were used for the calculation. From the slope of such a i_R vs i_D plot the value of $N = 0.18$ was obtained for the products oxidized at the ring at $+1.0$ V. Compared to the N value of 0.22, measured for the known stable ferrocene system, indicate that almost all of the intermediate species dissipate into the bulk solution and are not yet consumed at the disk electrode. This is in agreement with the proposition of quinodimethane as the intermediate, for which a relatively long lifetime (50% polymerized after 30 min at 20°C) has been reported.²⁴ The fraction of the intermediates that escape detection at the ring electrode depends on the rate of the follow-up reaction step and the time interval between the generation and detection of the intermediate. Accordingly a N value of 0.2 was obtained when using the data from Figure 3 with a higher rotation rate of 900 rpm. For the products oxidized at the ring electrode at $+1.3$ V a collection efficiency of 0.38 was obtained. This value suggests that two bromine atoms are split away during reduction of monomer **1** giving a two-electron ring response compared to the one-electron process for the Fe(CN)₆⁴⁻ system which gave a N value of 0.2. This finding is in accordance with the suggested reaction path for reduction of monomer **1** (A) shown in Scheme 1.

The plot of i_D^{-1} vs $\omega^{-1/2}$ (Levich-Koutecky plot) in Figure 4 for various disk potentials yields straight lines with intercepts corresponding to the inverse of the kinetic current, i_K , according to eq 1.¹⁷ The data used in Figure 4 were obtained from Figure 3.

$$\frac{1}{i_D} = \frac{1}{i_K} + \frac{1}{B\omega^{1/2}} \quad (1)$$

$$B = 0.62nFAcD^{2/3}\gamma^{-1/6} \quad (2)$$

$$i_K = nFAkc \quad (3)$$

$$k = k^0 e^{-\alpha nFE/RT} \quad (4)$$

In the equations F is the Faraday constant, n is the number of transferred electrons, A is the disk electrode area (0.328 cm^2), γ is the kinematic viscosity (viscosity/density, $0.8411 \times 10^{-2}\text{ cm}^2\text{ s}^{-1}$), k is the rate constant (cm s^{-1}), α is the transfer coefficient, and D and c are the diffusion coefficient ($1.9 \times 10^{-5}\text{ cm}^2\text{ s}^{-1}$) and the concentration ($0.05 \times 10^{-3}\text{ mol cm}^{-3}$) of monomer **1**, respectively.

The straight lines in Figure 4 do not go through the origin, indicating that there is a mixed kinetic-diffusion control of the reaction. The slope of the straight lines allows us, according to eq 2, to calculate the number of electrons involved in the reduction reaction of monomer **1**. Some of the kinetic parameters obtained from the Levich-Koutecky plots in Figure 4 are given in Table 1. The n values in Table 1 show that in the reduction of monomer **1** at least $2e^-$ are consumed in the first reduction wave. These values are in accordance with those obtained from the RRDE collection experiments.

The kinetic current, i_K , can be obtained from the y -axis intercepts in Figure 4 according to eq 1. Values of i_K were between 4×10^{-4} and $10 \times 10^{-4}\text{ cm s}^{-1}$. These

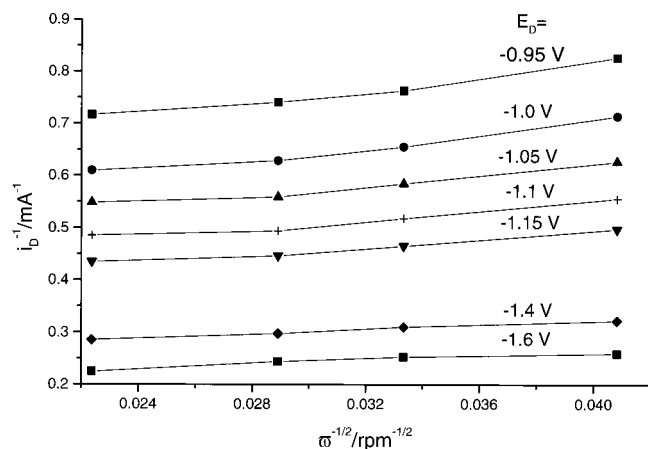


Figure 4. i_b^{-1} vs $\omega^{-1/2}$ plots as a function of different negative potentials applied to the disk in the study of electroreduction of monomer **1** in 0.1 M (TEA)BF₄-DMF.

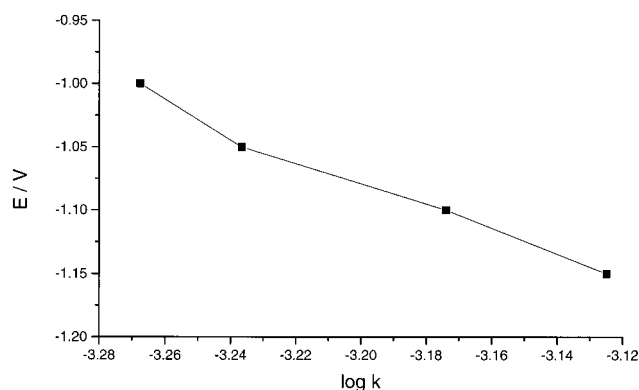


Figure 5. E vs $\log k$ plot obtained from the intercepts of Figure 4 for the reduction of monomer **1**.

Table 1. Kinetic Parameters from the RRDE Experiments for the Electrochemical Reduction of Monomer 1 in 0.1 M (TEA)BF₄-DMF

disk potential (V)	slope (mA ⁻¹ rpm ^{1/2})	intercept (mA ⁻¹)	<i>n</i>
-0.95	6.1	0.71	1.05
-1.0	5.7	0.59	1.1
-1.05	4.4	0.54	1.45
-1.1	3.9	0.47	1.64
-1.15	3.5	0.43	1.82
-1.4	2.2	0.28	2.25
-1.6	2.0	0.23	2.5

values can be used to calculate the rate constant, k , according to eq 3. When E is plotted vs $\log k$ according to eq 4, a straight line is observed as can be seen in Figure 5. The slope of that line is -110 mV/decade at 25 °C.

The obtained slope indicates that the reaction rate of the first reductive step is controlled by a one-electron-transfer step provided that $\alpha = 0.5$.¹⁷ This finding and the obtained n values shown in Table 1 are in favor of the mechanism involving a one-electron transition state in accordance with Scheme 1. For electrochemical reduction of organic halides a mechanism where one electron is added in the rate-determining step to produce a transition state in which the carbon atom has radical character has been suggested. The radicals formed from such a transition state can then participate in a fast further reduction process^{11,25} according to the mechanism shown in Scheme 1. It has also been shown that α -halo-*p*-xylyl anions do not eliminate the halogen ion

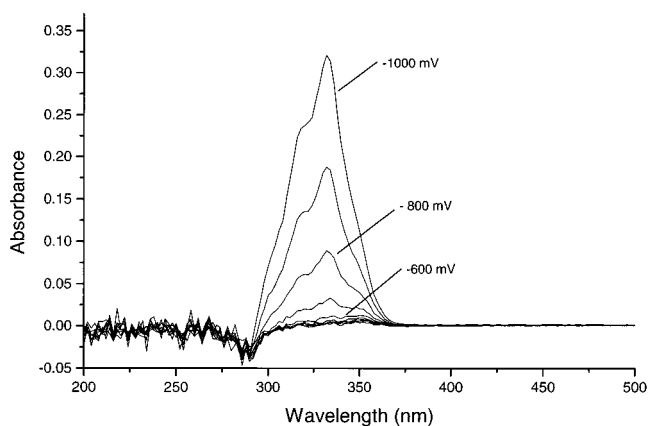


Figure 6. UV-vis spectra recorded during a potential scan experiment. Experimental parameters: 0.05 M monomer **1** in 0.1 M (TEA)BF₄ (DMF). The potential was scanned from 0 to -1.0 V using a 50 mV/s scan rate.

from the α -position and form carbenes but eject the halogen ion from the α' -position to yield the more stable xylenes.¹² The intermediate products formed during electroreductive polymerization of monomer **1** will be further studied by UV-vis-ESR spectroscopy.

3.1.2. In Situ UV-Vis-ESR Measurements. The in situ UV-vis spectra recorded at room temperature in the thin layer cell during the first potential cycle from 0 to -1.0 V in a solution of monomer **1** is shown in Figure 6. A UV-vis response began to appear after reaching the potential of -0.6 V, giving absorbance peaks at 318 and 332 nm and shoulders at 300 and 348 nm. During simultaneous ESR measurements no signal could be observed. In the RRDE experiments in Figure 2a, we could observe oxidation of bromide in the potential range -0.6 to -1.0 V. The bromide ion is splitted off when reducing monomer **1**. The absorbance peaks in Figure 6 are therefore interpreted to originate from species B and/or C shown in Scheme 1. Absorbance peaks have been reported for the *p*-(chloromethyl)benzyl radical at 320 nm and for *p*-xylylene at 290, 316, 331, and 349 nm,^{24,26,27} which are in agreement with those obtained in Figure 6.

When the potential cycle was extended to -2.3 V, during electrochemical polymerization of PPV, an ESR signal could be observed. The UV-vis spectra recorded during such a potential scan between 0 and -2.3 V and the ESR signal obtained at -2.3 V are shown in Figure 7. The intensity of the ESR signal increased during the reduction cycle after a potential of -1.6 V was reached and decreased again during the reverse scan. Changes in the UV-vis response can also be observed after reaching the potential of -1.6 V. These are the absorbance at 348 nm now seen as a peak and the weak broad absorbance response extending from 364 to 440 nm. During the reverse sweep of the first cycle, all of the peaks observed in wavelength range 300 to 364 nm will slowly decrease. However, an increase during the reverse sweep can be observed in the range from 364 to 440 nm. The line marked with stars in Figure 7 shows the absorbance response recorded at -230 mV during the reverse scan. The thick line at zero absorbance shows the response from a monomer free solution in the potential range used during the electrochemical polymerization reaction. If the working electrode was removed from the light beam path in the cell after the first reduction cycle, absorbance peaks at the same wavelength as in Figure 7 could be observed although they

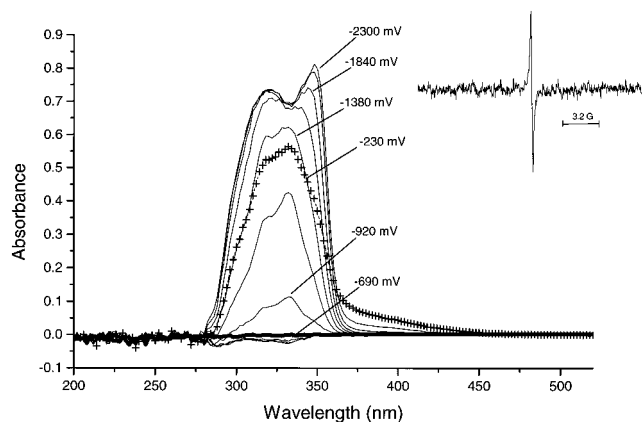


Figure 7. UV-vis spectra recorded during a potential scan between 0 and -2.3 V in 0.05 M monomer **1** in 0.1 M (TEA) BF_4 (DMF). 50 mV/s was used as the scan rate. The ESR signal obtained at -2.3 V is also shown.

were lower in intensity. This demonstrates that the species giving the absorbance response in Figure 7 are mostly from soluble intermediate products formed during electrochemical polymerization of PPV. According to ref 24, chlorinated *p*-xylylene intermediates have a relatively long lifetime, allowing detection. The solution species can therefore be assigned to short PPV oligomer chains not precipitated at the electrode and to brominated quinodimethane (C). Also a spontaneous reaction of brominated quinodimethane (C) to poly-*p*-xylylene (D) has been reported when using temperatures below 30°C .²⁸ In the RRDE experiments, we could observe the second bromine oxidation response at the same potential value (-1.6 V) at which the changes in the absorbance response in Figure 7 were obtained. This indicates that the peak at 348 nm probably is due to products formed after bromine is split away from the brominated quinodimethane intermediate. The fact that this absorbance response decreases during the reverse scan and that the broad response ranging from 364 to 440 nm increases indicates that the intermediates are consumed in follow-up reactions. The UV-vis spectra reported for PPV oligomer chains have shown a red shift of the π - π^* transition with an increasing number of monomer units (n).²⁹ For $n = 3$, a UV-vis response ranging from 330 to 430 nm and with a π - π^* transition at 386 nm has been reported. The absorption curve for chemically polymerized PPV gives a π - π^* transition at about 450 nm. We may therefore conclude that the broad UV-vis response ranging from 364 to 440 nm is due to follow-up reactions of the intermediates formed during the reduction of monomer **1** giving short oligomer chains of PPV. When looking at the cyclic voltammogram in Figure 1 showing the current response from the first polymerization cycle during electrochemical polymerization of PPV, we can observe that also an increase in the Faradaic current occurs at -1.6 V. In earlier work by our group, EQCM measurements demonstrated a mass increase at this potential value.¹⁰ Additionally, IR and Raman bands reported for chemically synthesized PPV were observed after reaching the potential of -1.6 V during the electrochemical polymerization of PPV.^{18,19}

If lower concentrations of monomer **1** are used it is possible to distinguish between the different absorbance peaks observed in Figure 7. In this case, the UV-vis method must be fast enough in order to observe fast reacting intermediates at low concentration. Therefore, a spectroelectrochemical UV-vis cell based on a litho-

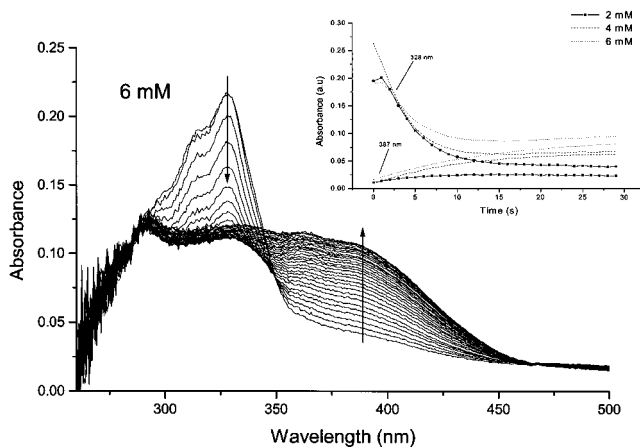


Figure 8. UV-vis spectra recorded after application of a constant potential of -1.0 V to the LIGA cell (2 s) containing 6 mM monomer **1** in 0.1 M (TEA) BF_4 (DMF). In the inset, the chronoabsorptometric curves obtained during the relaxation step following the application of -1.0 V for 2 s to the LIGA cell are shown. Solutions containing 2 , 4 , or 6 mM monomer **1** in 0.1 M (TEA) BF_4 (DMF) were used in the experiments.

graphic galvanic (LIGA) structure as working electrode in a capillary slit was used.¹⁶ The light beam passes through the hexagonal holes of the LIGA electrode, which allows the combination of electrochemical investigations with spectroscopy. The fast response time of the LIGA cell permits the study of fast chemical follow-up reactions so that even intermediates with a short lifetime can be detected. The UV-vis spectra recorded at different times after application of a constant potential of -1.0 V for 2 s to the LIGA cell containing 6 mM of monomer **1** is shown in Figure 8. The arrows indicate the direction of the absorbance change.

As can be seen in Figure 8 a decrease in absorbance with time was obtained at 298 , 316 , and 328 nm, while at 342 , 366 , and 387 nm an increase in the absorbance was observed. The interplay between gradual decreasing and increasing intensities of the UV-vis peaks at open circuit after applied potential indicates that there are intermediates present that in turn are involved in further reactions leading to formation of PPV oligomer chains. The increase in absorbance is directly dependent on the concentration of the monomer material (see inset in Figure 8). No absorbance response was detected in the wavelength range 200 – 500 nm when using monomer-free solutions, indicating that the peaks seen in Figure 8 result from intermediates formed during reduction of monomer **1**. In the LIGA cell the peaks responsible for the broad absorbance shoulder ranging from 364 to 440 nm in Figure 7 could be distinguished (seen at 342 , 366 , and 387 nm). For the biradical form of C, bands at 365 , 389 , and 418 nm have been reported.³⁰ These bands coincide nicely with the bands observed in the LIGA cell and confirms the presence of the biradical form of the intermediate *p*-xylylene (C) when monomer **1** is reduced. The obtained ESR signal can also be due to this biradical formation.

The absorbance, as a function of time recorded at wavelengths of 328 and 387 nm after application of -1.0 V for 2 s to the LIGA cell is shown as an inset in Figure 8. From the inset, it can clearly be observed that the concentration of monomer **1** has an influence on the amount of both intermediate (328 nm) and oligomer material (387 nm) produced. For the band at 328 nm, a tendency toward upward curvature can be observed

after 18 s when the concentration of monomer material was increased. This is due to the growth of a new peak at 342 nm, which will shift the baseline for the peak at 328 nm as well. This can be seen clearly in Figure 8.

When the temperature in the UV-vis-ESR experiments was decreased to $-10\text{ }^{\circ}\text{C}$ or when the LIGA cell was used, a much lower negative potential was needed (-1.3 and -1.0 V, respectively) to produce the same kind of UV-vis response as in Figure 7 (-2.3 V). The first UV-vis response, ranging from 300 to 330 nm, was however in all experiments, regardless of temperature or cell design, always obtained after reaching a potential of -0.6 V. Temperature does not, thus, strongly influence the first one-electron reduction process of monomer **1**. However, the shift in the reduction potential for the other reactions shows that lowering the temperature raises the efficiency of deposition, probably owing to a decrease in the solubility of the soluble oligomers. The larger surface area of the electrode and the geometry of the LIGA cell, which causes trapping of intermediates and prevents the diffusion of species before the critical chain length required for precipitation is reached, can be a reason for observing the shift of the reduction potential.

4. Conclusions

The RRDE and the in situ UV-vis-ESR techniques were applied to study the electropolymerization of PPV by reduction of monomer **1**. From the RRDE experiments a Br^- oxidation at $+1.2$ V was observed at the ring electrode. The observed dependence of the oxidation current of Br^- on the negative potential used for reduction of monomer **1**, the results obtained from the collection experiments, and the Levich-Koutecky plot lead to the conclusion that splitting of bromine from monomer **1** occurs in two steps. In the first reduction step, two bromide ions were removed. The UV-vis spectra confirmed the presence of brominated quinodimethane as an intermediate after the first reduction step. Upon further reduction (beyond -1.6 V), PPV oligomer chains were formed which precipitated at the electrode surface, giving an UV-vis response from 360 to 440 nm. This response was found to depend on the concentration of monomer **1**. The UV-vis response for the intermediate products formed when reducing monomer **1** was found to depend on the temperature and cell design. The same absorbance curves were obtained at -2.3 V at room-temperature conditions as at -1.3 V when the temperature was decreased to $-10\text{ }^{\circ}\text{C}$. A UV-vis response similar to that observed at -2.3 V could be observed already at -1.0 V by using a lithographic galvanic microstructured metal foil (LIGA) as the working electrode in a special UV-vis cell.

Acknowledgment. Financial support from the Deutsche Akademische Austauschdienst and from the Academy of Finland, Process Chemistry Group (Finnish Centre of Excellence Program 2000-2005) is gratefully acknowledged.

References and Notes

- (1) Burroughs, J. H.; Bradley, D. D. C.; Brown, A. R.; Marks, R. N.; Mackay, K.; Friend, R. H.; Burn, P. L.; Holmes, A. B. *Nature (London)* **1990**, *347*, 539.
- (2) Wessling, R. A. *J. Polym. Sci., Polym. Symp.* **1985**, *72*, 55.
- (3) Denton, F. R.; Sarker, A.; Lahti, P. M.; Garay, R. O.; Karasz, F. E. *J. Polym. Sci., Part A: Polym. Chem.* **1992**, *30*, 2233.
- (4) Heinze, J. In *Organic Electrochemistry*, 4th ed.; Lund, H., Hammerich, O., Eds.; Marcel Dekker: New York, 2001; p 1309.
- (5) Lang, P.; Chao, F.; Costa, M.; Garnier, F. *Polymer* **1987**, *28*, 668.
- (6) Raymond, D. E.; Harrison, D. J. *J. Electroanal. Chem.* **1990**, *296*, 269.
- (7) John, R.; Wallace, G. G. *J. Electroanal. Chem.* **1991**, *306*, 157.
- (8) Fauvarque, F.-C.; Digua, A.; Petit, M.-A.; Savard, J. *Makromol. Chem.* **1985**, *186*, 2415.
- (9) Damlin, P.; Kvarnström, C.; Ivaska, A. *Electrochim. Acta* **1999**, *44*, 4087.
- (10) Damlin, P.; Kvarnström, C.; Ivaska, A. *Anal. Chim. Acta* **1999**, *385*, 175.
- (11) Covitz, F. H. *J. Am. Chem. Soc.* **1967**, *89*, 5403.
- (12) Gilch, H. G. *J. Polym. Sci.* **1966**, *4*, 1351.
- (13) Lund, T.; Pedersen, S. U.; Lund, H.; Cheung, K. M.; Utley, J. P. H. *Acta Chem. Scand., Sect. B* **1987**, *41*, 285.
- (14) Utley, J. H. P.; Gao, Y.; Gruber, J.; Zhang, Y.; Munoz-Escalona, A. *J. Mater. Chem.* **1995**, *5*, 1837.
- (15) Petr, A.; Dunsch, L.; Neudeck, A. *J. Electroanal. Chem.* **1996**, *412*, 153.
- (16) Neudeck, A.; Dunsch, L. *J. Electroanal. Chem.* **1995**, *386*, 135.
- (17) Bard, A. J.; Faulkner, L. R. *Electrochemical Methods*; Wiley: New York, 1980.
- (18) Damlin, P.; Kvarnström, C.; Ivaska, A. *Synth. Met.* **2001**, *123*, 141.
- (19) Damlin, P.; Kvarnström, C.; Petr, A.; Ek, P.; Dunsch, L.; Ivaska, A. *J. Solid State Electrochem.*, in press.
- (20) Gutmann, V.; Duschek, O. *Monatsh. Chem.* **1973**, *104*, 654.
- (21) Asavapiriyamont, S.; Chandler, G. K.; Gunawardena, G. A.; Pletcher, D. *J. Electroanal. Chem.* **1984**, *177*, 229.
- (22) Nofle, R. E.; Pletcher, D. *J. Electroanal. Chem.* **1987**, *227*, 229.
- (23) Raymond, D. E.; Harrison, D. J. *J. Electroanal. Chem.* **1993**, *361*, 65.
- (24) Gilch, H. G. *Angew. Chem., Int. Ed. Engl.* **1965**, *4*, 598.
- (25) Rifi, M. R. In *Organic Electrochemistry*; Baizer, M. M., Ed.; Marcel Dekker: New York and Basel, Switzerland, 1973; p 279.
- (26) Miranda, M. A.; Perez-Prieto, J.; Font-Sanchis, E.; Scaiano, J. C. *Chem. Commun.* **1998**, 1541.
- (27) Kaupp, G. *Angew. Chem., Int. Ed. Engl.* **1976**, *15*, 442.
- (28) Gorham, W. F. *Polym. Sci.: Part A-1* **1966**, *4*, 3027.
- (29) Tian, B.; Zerbi, G.; Schenk, R.; Müllen, K. *J. Chem. Phys.* **1991**, *95*, 3191.
- (30) Subhan, W.; Rempala, P.; Sheridan, R. S. *J. Am. Chem. Soc.* **1998**, *120*, 11528.

MA0118116